



# Coupling of proton flow to ATP synthesis in *Rhodobacter capsulatus*: $F_0F_1$ -ATP synthase is absent from about half of chromatophores

Boris A. Feniouk<sup>a, b</sup>, Dmitry A. Cherepanov<sup>a, c</sup>, Wolfgang Junge<sup>a</sup>,  
Armen Y. Mulkidjanian<sup>a, b, \*</sup>

<sup>a</sup> Division of Biophysics, Faculty of Biology/Chemistry, University of Osnabrück, D-49069 Osnabrück, Germany

<sup>b</sup> A.N. Belozersky Institute of Physico-Chemical Biology, Moscow State University, Moscow 119899, Russia

<sup>c</sup> Institute of Electrochemistry, Russian Academy of Sciences, Leninskii prosp. 31, 117071 Moscow, Russia

Received 8 May 2001; received in revised form 10 August 2001; accepted 13 August 2001

## Abstract

$F_0F_1$ -ATP synthase ( $H^+$ -ATP synthase,  $F_0F_1$ ) utilizes the transmembrane protonmotive force to catalyze the formation of ATP from ADP and inorganic phosphate ( $P_i$ ). Structurally the enzyme consists of a membrane-embedded proton-translocating  $F_0$  portion and a protruding hydrophilic  $F_1$  part that catalyzes the synthesis of ATP. In photosynthetic purple bacteria a single turnover of the photosynthetic reaction centers (driven by a short saturating flash of light) generates protonmotive force that is sufficiently large to drive ATP synthesis. Using isolated chromatophore vesicles of *Rhodobacter capsulatus*, we monitored the flash induced ATP synthesis (by chemoluminescence of luciferin/luciferase) in parallel to the transmembrane charge transfer through  $F_0F_1$  (by following the decay of electrochromic bandshifts of intrinsic carotenoids). With the help of specific inhibitors of  $F_1$  (efrapeptin) and of  $F_0$  (venturicidin), we decomposed the kinetics of the total proton flow through  $F_0F_1$  into (i) those coupled to the ATP synthesis and (ii) the de-coupled proton escape through  $F_0$ . Taking the coupled proton flow, we calculated the  $H^+$ /ATP ratio; it was found to be  $3.3 \pm 0.6$  at a large driving force (after one saturating flash of light) but to increase up to  $5.1 \pm 0.9$  at a smaller driving force (after a half-saturating flash). From the results obtained, we conclude that our routine chromatophore preparations contained three subsets of chromatophore vesicles. Chromatophores with coupled  $F_0F_1$  dominated in fresh material. Freezing/thawing or pre-illumination in the absence of ADP and  $P_i$  led to an increase in the fraction of chromatophores with at least one de-coupled  $F_0(F_1)$ . The disclosed fraction of chromatophores that lacked proton-conducting  $F_0(F_1)$  (approx. 40% of the total amount) remained constant upon these treatments. © 2001 Elsevier Science B.V. All rights reserved.

**Keywords:** Proton transfer; ATP synthesis; Electrochromism; Membrane potential; *Rhodobacter capsulatus*

Abbreviations: DCCD, *N,N'*-dicyclohexylcarbodiimide; DTT, dithiothreitol; EDTA, ethylenediaminetetraacetic acid;  $P^+$ , oxidized state of the primary electron donor in the photosynthetic reaction center; FWHM, full-width half-maximum; RC, photosynthetic reaction center of purple phototrophic bacteria; DMF, dimethylferrocene; BSA, bovine serum albumin;  $P_i$ , inorganic phosphate

\* Corresponding author. Fax: +49-541-969-2870.

E-mail address: [mulkidjanian@biologie.uni-osnabrueck.de](mailto:mulkidjanian@biologie.uni-osnabrueck.de) (A.Y. Mulkidjanian).

## 1. Introduction

$F_0F_1$ -ATP synthase ( $H^+$ -ATP synthase,  $F_0F_1$ ) is the key enzyme in energy transduction. It either synthesizes ATP using the transmembrane electrochemical potential difference of the proton ( $\Delta\tilde{\mu}_{H^+}$ ), or vice versa, it generates  $\Delta\tilde{\mu}_{H^+}$  by ATP hydrolysis (see [1–3] for recent reviews). Structurally the enzyme consists of two multisubunit portions. The membrane  $F_0$  portion (a complex of  $a_1b_2c_{10-14}$  subunits in bacteria) translocates protons. The hydrophilic  $F_1$  portion (a complex of  $\alpha_3\beta_3\gamma_1\delta_1\epsilon_1$  subunits) protrudes about 100 Å from the membrane and catalyzes the synthesis/hydrolysis of ATP. These portions are connected by two ‘stalks’ that are formed by the centrally located  $\gamma\epsilon$ -complex and by the eccentric  $b_2$  dimer (for the latest structural reviews see [4–7]).

ATPase is a rotary machine: evidence for the ATP hydrolysis-coupled movement of the  $\gamma_1\epsilon_1c_{10-14}$  complex (the rotor) inside the  $\alpha_3\beta_3$  ring (that together with  $a_1b_2\delta_1$  forms the stator) were obtained by using cleavable crosslinks [8,9], by polarized photochemistry [10], and by microscopic observations of the rotation of a fluorescent actin filament attached to the  $\gamma$  subunit of  $F_1$  [11]. Mechanism for torque generation by proton flow and for the coupling of proton transfer to ATP synthesis has been proposed, e.g., in [2,12,13].

Both elements,  $F_0$  and  $F_1$ , are likely rotary steps. The mismatch between the 3-fold pseudosymmetry in  $F_1$  and 10–14-fold symmetry in the  $c$ -oligomer ring implies some kind of elasticity inherent to the enzyme coupling machinery, as has been suggested in [2,14].

In photosynthetic systems an excitation by a short flash of light leads to the prompt generation of membrane protonmotive force. Thereby the membrane  $\Delta\tilde{\mu}_{H^+}$ -dependent enzymes, including the ATP synthase, can be studied in a light-triggered mode [15–19]. Recently we applied this approach to native membrane vesicles (chromatophores) isolated from a purple phototrophic bacterium *Rhodobacter capsulatus* [20]. Thereby we combined the technique of the complete tracking of proton flow developed for chloroplast ATP synthase [19], with the quantitative monitoring of the flash-induced ATP release. The proton transfer across the membrane was traced by

the electrochromism of membrane carotenoids [15,21,22] and by pH-indicators [23–25]. The flash-induced ATP yield was measured by luciferin-luciferase [17,26]. In agreement with previous observations for *Rhodobacter sphaeroides* [24], we discriminated two components in the proton flow related to  $F_0F_1$ : one component was induced by simultaneous addition of ADP and inorganic phosphate ( $P_i$ ) and was inhibited by efrapeptin, a potent  $F_1$  inhibitor. The second component was present even in the absence of ADP and  $P_i$ , and was insensitive to efrapeptin, but was inhibited by specific inhibitors of  $F_0$  (venturicidin, DCCD or oligomycin) [20].

It is noteworthy that the apparent kinetics of proton escape through  $F_0F_1$  might be influenced by the non-uniformity of the sample that, in the particular case of chromatophore vesicles, could have a dual origin. First, the coupling of proton transfer to the ATP synthesis can vary from a tight one to a loose one leading to a difference in the kinetics of proton transfer (see [27] for the respective studies on chloroplast thylakoids). The second type of possible inhomogeneity is specific to membrane vesicles that are as small as chromatophores. Their typical diameter is only about 60 nm [28], much smaller than those of submitochondrial particles or chloroplast thylakoids, so that each chromatophore might contain just a few, if any, ATP synthases. Then, at low numbers of ATP synthases per chromatophore, the kinetics of proton escape through  $F_0F_1$  might essentially vary from vesicle to vesicle and cause a kinetic inhomogeneity of the type that is absent in larger membrane vesicles (see [29] for a general discussion of the smallness-effects in chromatophores).

To determine the impact of the chromatophore non-uniformity on the coupling, we monitored here the proton flow through  $F_0F_1$  in parallel to the ATP synthesis in variously treated samples. Thereby we determined the properties and kinetic features of the coupled, ‘useful’ proton flow, leading to the synthesis of ATP, as well as of the de-coupled, ‘futile’ proton transfer. For the coupled proton transfer, we determined that  $H^+/ATP$  ratio was about  $3.3 \pm 0.6$  at large driving force but increased up to  $5.1 \pm 0.9$  at smaller driving force. We also found out that about 40% of chromatophores in our preparations did not contain proton-conducting  $F_0(F_1)$  at all.

## 2. Materials and methods

### 2.1. Cell growth and chromatophore preparation

Cells of *Rb. capsulatus* (wild-type, strain B10) were grown photoheterotrophically on malate as a carbon source at +30°C [30]. The light intensity was 18 W/m<sup>2</sup>. Cells were harvested at the logarithmic growth phase, washed twice with 30 mM HEPES–KOH (pH 7.4), 5 mM MgCl<sub>2</sub>, 0.5 mM DTT, 50 mM KCl, 10% sucrose and resuspended in the same pH-buffer. A few flakes of DNase were added. The cells were disrupted by sonication (Branson Sonifier B15, 4–5 exposures for 15 s with 1 min incubation on ice in between), and centrifuged (20 000 × *g*, 20 min, 4°C) to remove large cell fragments. The pellet was suspended in the same pH-buffer and re-sonicated as above; the re-sonicated suspension was centrifuged again (20 000 × *g*, 20 min, 4°C). Supernatants were collected and centrifuged (180 000 × *g*, 90 min, +4°C). The pellet was resuspended in 30 mM HEPES–KOH (pH 7.4), 5 mM MgCl<sub>2</sub>, 0.5 mM DTT, 50 mM KCl, 20% sucrose. It contained chromatophores at bacteriochlorophyll concentration of 0.3–0.7 mM. Chromatophores were stored at –80°C until use. In some experiments ‘freshly prepared’ chromatophores were used immediately after the preparation or, otherwise, were kept at +4°C overnight and used the next morning. The concentration of bacteriochlorophyll in the samples was determined spectrophotometrically in the acetone/methanol extract at 772 nm according to [31]. The amount of functionally active RCs was estimated from the extent of flash-induced absorption changes at 603 nm as in [32].

### 2.2. Preparation of chromatophores stripped of *F*<sub>1</sub>

Chromatophores were depleted of *F*<sub>1</sub> by EDTA-treatment [33–35]. Chromatophores from frozen stock were thawed and diluted 25-fold with 1 mM EDTA (pH 8) in daylight. The suspension was sonicated 5 times for 20 s with 1-min interval (on ice) and centrifuged at 180 000 × *g*, 90 min, +4°C. The pellet was resuspended in a medium containing 20 mM HEPES–KOH (pH 7.4), 5 mM MgCl<sub>2</sub>, 0.5 mM DTT, 50 mM KCl to yield a bacteriochlorophyll

concentration of 0.3–0.7 mM and used on the same day or after storage at +4°C overnight.

### 2.3. Spectrophotometric measurements

The kinetic flash-spectrophotometer was constructed according to [36]. Monitoring light was provided by a 200-W halogen lamp, and was heat-filtered (KG 2 filter, Schott, Mainz). The desired wavelengths were cut out by appropriate interference filters (Schott). A shutter was placed in front of the cuvette to eliminate the actinic effect of the monitoring beam between the measurements. The delay time between the opening of the shutter and the actinic flash was 400 ms. Changes in transmitted light intensity ( $\Delta I$ ) were monitored by a photomultiplier (Thorn EMI, 9801B) shielded with two blue filters (BG 39, Schott) from the actinic flash. The DC-output from the photomultiplier was pre-set to 1 V (load resistor: 10 k $\Omega$ ) by varying the current on the photomultiplier power supply. The photomultiplier output was connected to the positive input of a difference amplifier (Tektronix AM502). Before an actinic flash was fired, the signal was sampled and held by a home-made amplifier (designed and constructed by N. Spreckelmeier) connected to the negative input of the difference amplifier. The difference signal was amplified 100-fold, digitized and stored by an averaging oscilloscope (Nicolet, Pro 10). The analogue bandshift width was 3 kHz and the digital time-per-address was 200  $\mu$ s. The optical path was 1 cm, both for the exciting and for the measuring beam. The final concentration of bacteriochlorophyll in the cuvette was 8–12  $\mu$ M.

Repetitive signals measured at 0.08 Hz were averaged. The dark adaptation time of 12 s between flashes was chosen to allow the decay of transmembrane electrical potential difference ( $\Delta\psi$ ). This time was still short enough to prevent the de-activation of the *F*<sub>0</sub>*F*<sub>1</sub>-ATP synthase (the expected lifetime of the  $\Delta\psi$ -activated state of the *F*<sub>0</sub>*F*<sub>1</sub>-ATP synthase under conditions of our experiments was 30–70 s [37]).

Electrochromic carotenoid bandshifts at 522 nm were used to monitor  $\Delta\psi$  [21,22,38,39]. Notably, up to 15% of the flash-induced response was due not to the delocalized  $\Delta\psi$ , but to local electrochromic band-

shift (presumably in response to the  $P^+$  formation) that was insensitive to uncouplers.

Saturating actinic flashes were provided by a xenon flash lamp (FWHM approx. 10  $\mu$ s, the flash energy density on the cuvette was 12 mJ/cm<sup>2</sup>). A red optical filter (RG 780, Schott) covered the flash. Excitation by the xenon lamp flash gave 8–11% greater signals than a laser pulse (duration < 100 ns), indicating double turnover in about 10% of RCs, in agreement with the recent report on the presence of a 3- $\mu$ s component in the kinetics of the  $Q_B$  reduction in chromatophores of *Rb. sphaeroides* and *Rb. capsulatus* [40]. Because the deviation from single turnover conditions was not pronounced, we used the more convenient xenon flash in our experiments, correcting the calculations by 10%.

#### 2.4. ATP synthesis

ATP synthesis was monitored by chemoluminescence of luciferin–luciferase [26] in the same sample that was used for measurements of absorption changes. The photomultiplier was shielded against actinic light by a stack of three blue filters (BG 39, Schott). Aliquots of 0.5 mM freshly prepared ATP solution were added to up to 2  $\mu$ M final concentration for calibration; linear calibration curves were obtained in the range from 0.05 to 2  $\mu$ M ATP. The traces were corrected for linear drift due to the ATP hydrolysis (2–120 nM/min).

#### 2.5. Incubation medium

The samples were suspended in a medium which contained 50 mM KCl, 0.3% bovine serum albumin (BSA, was used as a pH-buffer), 5 mM MgCl<sub>2</sub>, 2 mM succinate/2 mM fumarate (as a redox buffer), 5 or 10  $\mu$ M DMF (as a redox mediator) and 2 mM KCN (to prevent the oxidation of the redox-buffer by the terminal oxidase). In some experiments 2 mM K<sub>4</sub>Fe[CN]<sub>6</sub> was present instead of succinate–fumarate redox buffering system. When ATP synthesis was measured, 8  $\mu$ g/ml luciferase and 0.2 mM luciferin were present in the medium.

### 3. Results

#### 3.1. Two types of proton conduction via $F_0F_1$ -ATP synthase

Fig. 1A shows typical absorption transients at 522 nm in a suspension of *Rb. capsulatus* chromatophores in response to a saturating actinic flash. Chromatophores were stored frozen at  $-80^\circ\text{C}$  in a medium containing 50% glycerol, and were thawed immediately before the measurement. The transients at 522 nm were due to the electrochromic bandshift of the membrane carotenoids and reflected the changes in the transmembrane electrical potential difference ( $\Delta\psi$ ). A minor, here unspecified contribution from local electrochromic bandshifts (up to 15% of the total response, see Materials and Methods) was also present at this wavelength.

A flash of light caused a fast biphasic increase in  $\Delta\psi$  due to the sequential operation of the photosynthetic reaction center (RC) and the cytochrome- $bc_1$  complex (ubiquinol:cytochrome  $c_2$  oxidoreductase). Electrogenic reactions in the RC included (i) electron transfer from the light-excited bacteriochlorophyll dimer  $P$  to the ubiquinone electron acceptors on the other side of the membrane ( $\sim 200$  ps); (ii) the reduction of the oxidized  $P^+$  by water soluble cytochrome  $c$  (3–150  $\mu$ s); and (iii) the trapping of one proton, on average, by the secondary quinone  $Q_B$  (100  $\mu$ s under our experimental conditions). Correspondingly, the fast, here unresolved component of  $\Delta\psi$  generation reflected the transfer of one electron per RC across the whole chromatophore membrane. The slower component of the  $\Delta\psi$  increase at millisecond time scale reflected the electrogenic oxidation of ubiquinol to ubiquinone by the cytochrome- $bc_1$  complex (see [18,41] for reviews on electrogenic reactions in chromatophores).

The following decay of the light-induced voltage transients at 522 nm was markedly accelerated by the addition of ADP and inorganic phosphate ( $P_i$ , see Fig. 1A, trace 2), in agreement with previous observations with chromatophores of *Rb. sphaeroides* [15,16]. The effect of ADP+ $P_i$  was reversed by efrapeptin, a peptide inhibitor that binds between sub-

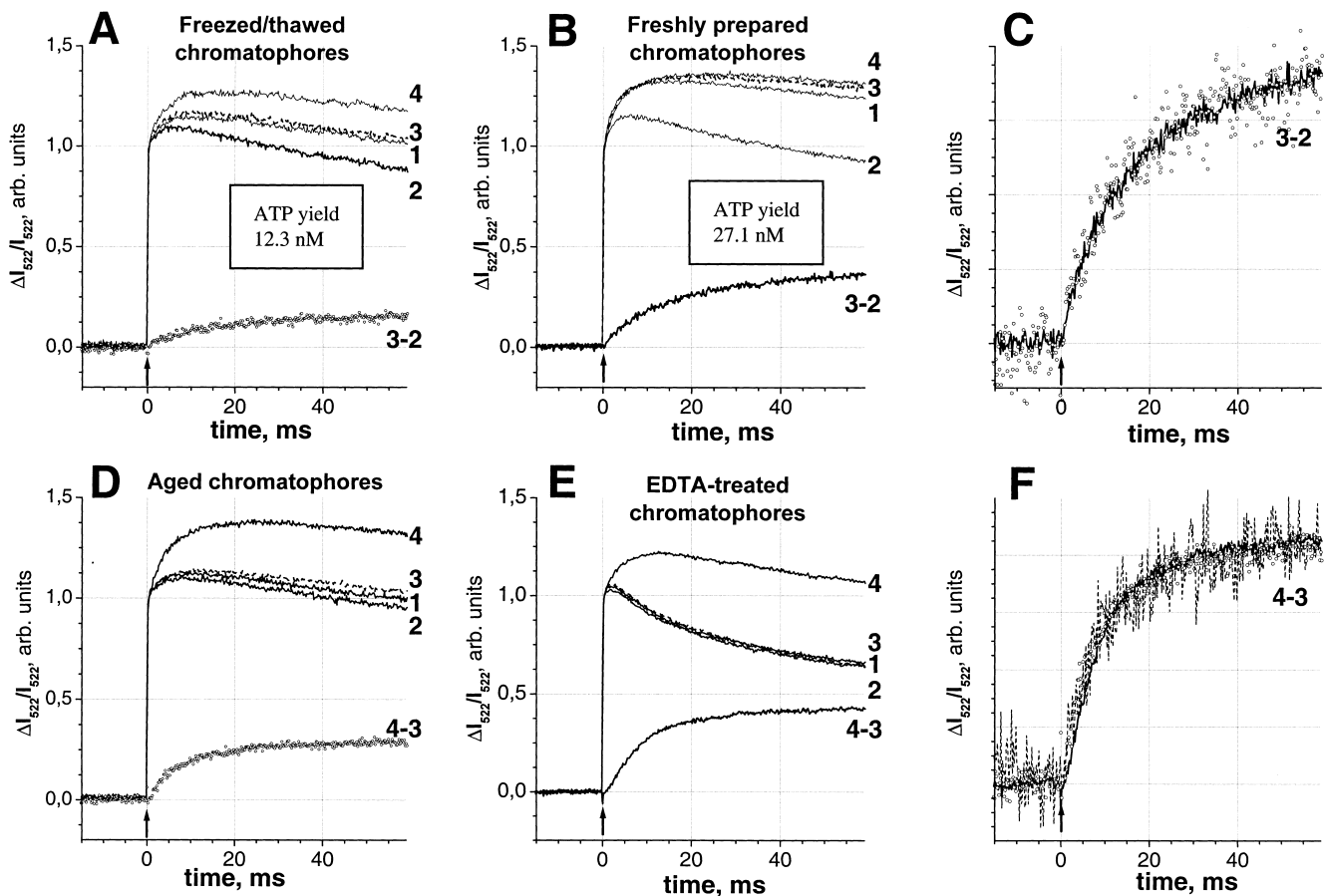


Fig. 1. Effect of freezing and storage on the components of proton transport through ATP synthase. Changes in absorption at 522 nm reflect changes in  $\Delta\psi$ , which, in turn, are linearly proportional to the net transmembrane charge transfer. Measuring medium contained 2 mM  $K_2HPO_4$ , 2 mM  $K_4[Fe(CN)_6]$ , 5  $\mu$ M DMF, 2 mM KCN, 5 mM  $MgCl_2$ , 50 mM KCl, 0.3% BSA, pH 7.9. Arrows mark actinic flashes. Same trace numeration is used in all panels: 1, no additions; 2, ADP to 400  $\mu$ M; 3, ADP to 400  $\mu$ M, efrapeptin to 200 nM; 4, ADP to 400  $\mu$ M, efrapeptin to 200 nM, venturicidin to 200 nM. Difference trace  $\pm$  efrapeptin and  $\pm$  venturicidin are marked 3-2 and 4-3, respectively. (A) Chromatophores stored 1 week at  $-80^\circ\text{C}$  in a pH-buffer containing 50% glycerol. (B) Freshly prepared chromatophores. (C) Difference traces ( $\pm$  efrapeptin) for A and B samples scaled to compare the kinetics (scaling factor: 2.4). (D) Chromatophores as in B but stored in the measuring medium overnight at  $+4^\circ\text{C}$ . (E) EDTA-treated,  $F_1$ -stripped chromatophores. (F) Difference traces ( $\pm$  venturicidin) for A, D and E samples scaled to compare the kinetics (scaling factors: 3.23 (A), 1.48 (D)).

unit  $\gamma$  and the  $\alpha_3\beta_3$  hexamer in  $F_1$  [42] (Fig. 1A, trace 3). The inhibitor decreased the decay rate of the light-induced voltage transients approximately to the level that was observed in the absence of ADP and  $P_i$ . A further slowing of the voltage decay was achieved when the inhibitors of proton conduction through the  $F_0$ -portion of ATP synthase, namely venturicidin, oligomycin, or DCCD [43,44], were added *over* efrapeptin (Fig. 1A, trace 4 compared to trace 3). The former inhibitors decreased the decay rate also when they were added in the absence of ADP or phosphate (see e.g. [20]). The maximal inhi-

bition by the  $F_0$ -inhibitors was observed at the following incubation times: from 20 to 90 min for DCCD (depending on pH), 15 min for oligomycin, and 1–2 min for venturicidin. Because of its efficiency, we mostly used venturicidin throughout this work.

Previously, by combining hydrophilic and amphiphilic pH-indicators, we showed that the membrane discharge is due to the  $\Delta\tilde{\mu}_{H^+}$ -driven proton escape from the chromatophore lumen through  $F_0F_1$  [20]. The ADP+ $P_i$ -induced voltage discharge that was sensitive to efrapeptin could be then attributed provi-

sionally to the ‘useful’ proton transfer through the  $F_0F_1$ -ATP synthase, coupled to the ATP synthesis, whereas the surplus venturicidin-sensitive discharge to some kind of a non-coupled, ‘futile’ proton flow.

We found out that the relative extent of the  $ADP+P_i$ -induced component of proton flow depended on the choice of cryoprotector for the chromatophore storage. When chromatophores were routinely frozen in a pH-buffer containing 50% (v/v) glycerol, the  $ADP+P_i$ -induced and the ‘futile’ components of proton transfer were approximately equal in magnitude (Fig. 1A). Among other cryoprotectors tested (DMSO, ethylene glycol, ficoll, sucrose, and glycerol) sucrose (25%) was the most efficient in maintaining the  $ADP+P_i$ -induced proton flow. Notably, if the chromatophores were not frozen at all, the ‘futile’ proton transfer was very small if not negligible (Fig. 1B).

The time course of the  $ADP+P_i$ -induced proton discharge was obtained by subtraction of kinetic traces measured in the presence of  $ADP+P_i$  from those recorded in the presence of efrapectin. The respective difference traces obtained both from Fig. 1A (frozen/thawed sample) and Fig. 1B (fresh sample) are plotted in Fig. 1C after scaling their amplitudes. Although the absolute extents differed by a factor of two (see the figure legend), the discharge characteristic times were equal, of about 20 ms (compare the two data sets in Fig. 1C).

Cold storage of chromatophores at +4°C overnight, eventually, abolished the sensitivity of the voltage discharge both to  $ADP+P_i$  and to efrapectin. The sensitivity to venturicidin, however, remained (see Fig. 1D). Apparently, upon freezing/thawing or ageing of chromatophore preparation, the extent of the ‘futile’ component of proton transport through ATP synthase increased at the expense of the  $ADP+P_i$ -inducible, efrapectin-sensitive component.

We compared the kinetics of proton transfer through the ATP synthase in chromatophores that were stored overnight at 4°C (Fig. 1D) with those in chromatophores that were depleted in  $F_1$  by the EDTA treatment plus sonication (Fig. 1E). According to this well established technique (see [33–35]), such a treatment yields approximately 85%  $F_1$  depletion. In the chromatophores treated in such way the proton flow was insensitive both to  $ADP+P_i$  addition

and to efrapectin, but was sensitive to venturicidin (Fig. 1E).

The traces in Fig. 1F represent the scaled difference traces between the voltage transients obtained in the presence of venturicidin and those obtained in the presence of efrapectin, with frozen/thawed, aged, and EDTA-stripped chromatophores. In the case of freshly prepared chromatophores this difference was negligible. In all the preparations the ‘futile’ proton transfer kinetics had the same time constant of approximately 10 ms.

The pattern of the overall  $\Delta\psi$  decay in the presence of venturicidin was more or less the same in all experiments and was independent of the presence of ADP, phosphate, efrapectin or chromatophore storage conditions (see Fig. 1A,B,D,E).

### 3.2. ATP synthesis in various chromatophore preparations

We determined the amount of ATP that was synthesized after a flash excitation in differently treated chromatophore preparations. The extent of luminescence transients of luciferin–luciferase was proportional to the yield of ATP per flash, but its time course did not truly reflect the kinetics of ATP synthesis, because of a  $\sim 100$ -ms lag in the luminescence increase [45]. The respective ATP-yields are given in the boxes in Fig. 1A,B. The amount of ATP synthesized was maximal in freshly prepared, non-frozen chromatophores (Fig. 1B). It was less in chromatophores that were frozen and kept at  $-80^\circ\text{C}$  after the preparation (Fig. 1A). In chromatophores that were stored overnight at 4°C (Fig. 1D) or in the  $F_1$ -depleted chromatophores (Fig. 1E), the ATP yield after a single flash, if any, was below the resolution of our luminometer. In a series of similar experiments we found out that the relative yield of ATP was proportional to the relative extent of the  $ADP+P_i$ -induced and efrapectin-sensitive, ‘useful’ charge transfer.

### 3.3. The effect of pre-illumination in the absence of ADP and $P_i$ on proton transfer and ATP synthesis

The pre-illumination of chromatophores in the absence of ADP led to an increase in the proton flux through  $F_0F_1$  as it followed from the acceleration of

$\Delta\psi$  decay (Fig. 2A). Applying specific inhibitors of  $F_1$  and  $F_0$  (efrapeptin and venturicidin, respectively) to such pre-illuminated chromatophores, we revealed that the  $\Delta\psi$  decay acceleration was due to the increase in the ‘futile’ component of proton transfer at the expense of the coupled, i.e., ADP+ $P_i$ -induced and efrapeptin-sensitive, component. Pre-illumination by red light for 20 s was sufficient to almost totally abolish the ADP+ $P_i$ -induced component (see traces 1 and 2 in Fig. 2A).

When ADP was added to the pre-illuminated sample, a gradual recovery of the ADP+ $P_i$ -induced, efrapeptin-sensitive component was observed. When efrapeptin was added 30 min after ADP, the decrease in the rate of  $\Delta\psi$  decay was pronounced, although it had not reached the level of the initial control trace (compare traces 3, 4 and 1 in Fig. 2A). However, if efrapeptin was added immediately after the trace with ADP was recorded, no significant slowing of the  $\Delta\psi$  decay was observed, so that the pattern resembled those in Fig. 1D (not documented).

ATP synthesis, as measured by luciferin–luciferase luminescence, was also reduced to about 35% of the control, when the sample was pre-illuminated by red light before ADP was added (Fig. 2B). In this case, however, there was always a dead time of about 5 min after ADP addition that was necessary for the sample equilibration before the measurement. We believe that the partial recovery of the enzyme during the 5-min incubation in the presence of ADP+ $P_i$  accounted for the notable ATP yield in the pre-illuminated sample. The recovery was even

more pronounced when the post-illumination incubation was prolonged for 30 min: the ATP synthetic activity was restored up to 70% of the control level (Fig. 2B).

### 3.4. Dependence of the ATP synthesis on the flash intensity

We studied how the coupled, ADP+ $P_i$ -sensitive proton transfer and the ATP yield depended on the transmembrane voltage. To vary the latter, we decreased the intensity of the actinic flash by mounting neutral density optical filters on it. Fig. 3 shows that when the actinic flash was attenuated so that  $\Delta\psi$  generation dropped about 2-fold, the ‘useful’ proton transfer through ATP synthase decreased by a factor of  $\sim 2.4$ , whereas the drop in ATP yield was, on average, more than 4-fold. Table 1 summarizes the data from several experiments.

### 3.5. Proton transfer via $F_0$ after two subsequent flashes of light

As could be seen in Fig. 1C, the kinetics of proton discharge sensitive to ADP+ $P_i$  and to efrapeptin had a time constant of about 20 ms [20]. Then one would expect that  $\Delta\psi$  decayed almost to zero in approx. 100 ms. Still  $\Delta\psi$  remained significant even 200 ms after the flash in the presence of ADP and phosphate, i.e., under ATP synthesis conditions (Fig. 4A). By analogy with plant thylakoids [46], we had previously attributed this phenomenon to the  $\Delta\psi$  threshold of

Table 1  
Yield of ATP and the amount of protons transferred through ATP synthase in dependence on flash intensity

Expt. no.	Full flash $\Delta\psi_{RC}$ Weak flash $\Delta\psi_{RC}$	$R_{\text{protons}} = \frac{\text{Full flash } \Delta\psi_{\text{Efra}}}{\text{Weak flash } \Delta\psi_{\text{Efra}}}$	$R_{\text{ATP}} = \frac{\text{Full flash } \Delta C_{\text{ATP}}}{\text{Weak flash } \Delta C_{\text{ATP}}}$	$\frac{R_{\text{ATP}}}{R_{\text{protons}}}$
1	2.44	2.94	4.80	1.63
2	2.35	2.72	3.72	1.37
3	2.27	2.42	3.43	1.42
4	2.32	2.70	4.69	1.74
5	2.59	3.71	4.32	1.36
6	2.18	2.38	4.96	2.08
Average	$2.36 \pm 0.14$	$2.81 \pm 0.49$	$4.32 \pm 0.62$	$1.60 \pm 0.28$

Full flash  $\Delta\psi_{RC}$  and Weak flash  $\Delta\psi_{RC}$  denote the extent of the fast  $\Delta\psi$  generation component attributed to charge separation in the reaction centers after a saturating and an attenuated flash, respectively. Full flash  $\Delta\psi_{\text{Efra}}$  and Weak flash  $\Delta\psi_{\text{Efra}}$  denote the extent of the charge transfer through ATP synthase that is sensitive to efrapeptin; their ratio  $R_{\text{protons}}$  reflects a relative decrease in this transfer after flash attenuation. Full flash  $\Delta C_{\text{ATP}}$  and Weak flash  $\Delta C_{\text{ATP}}$  denote the increase in ATP concentration; their ratio  $R_{\text{ATP}}$  reflects relative decrease in ATP yield after flash attenuation.

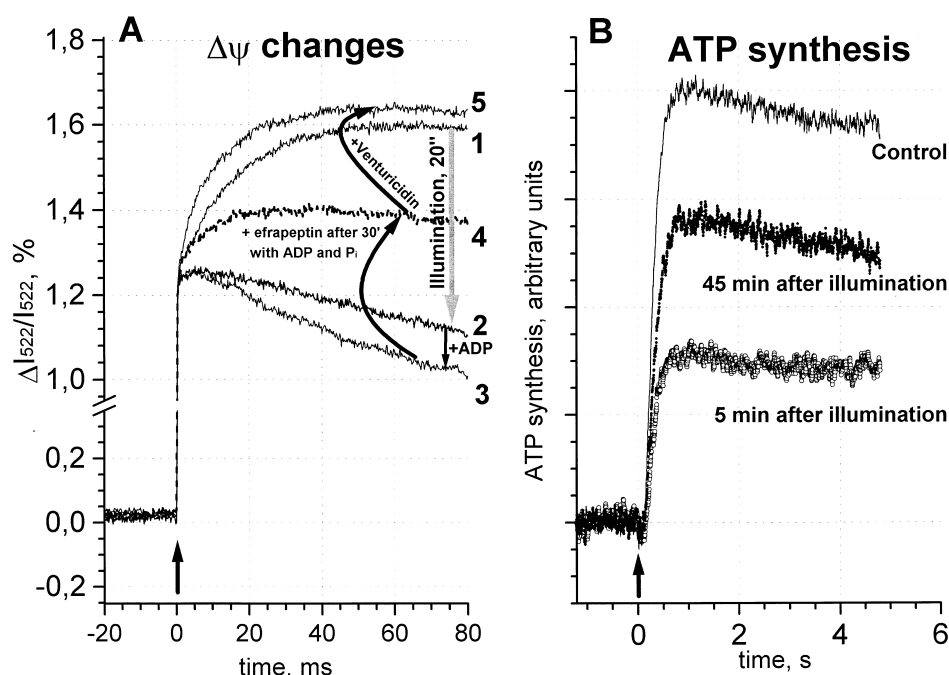


Fig. 2. Effect of the far-red pre-illumination on proton transfer and ATP synthesis. Arrows indicate light flashes. (A) Flash-induced absorption changes at 522 nm. Traces were consequently recorded in the same cuvette. 1, control trace; 2, 10 min after illumination of the sample for 20 s with far-red light; 3, immediately after ADP was added to 30  $\mu$ M; 4, after 30 min dark incubation with ADP followed by the addition of efrapentin (250 nM); 5, after venturicidin (200 nM) was added. Note the y-axis break. (B) ATP synthesis as measured 5 min and 45 min after a far-red pre-illumination followed by an addition of ADP (30  $\mu$ M) as compared with a non-illuminated sample. Measuring medium contained 2 mM  $K_2HPO_4$ , 2 mM  $K_4[Fe(CN)_6]$ , 5  $\mu$ M DMF, 2 mM KCN, 5 mM  $MgCl_2$ , 50 mM KCl, 0.3% BSA, pH 7.9; 8  $\mu$ g/ml luciferase and 0.2 mM luciferin were present in B.

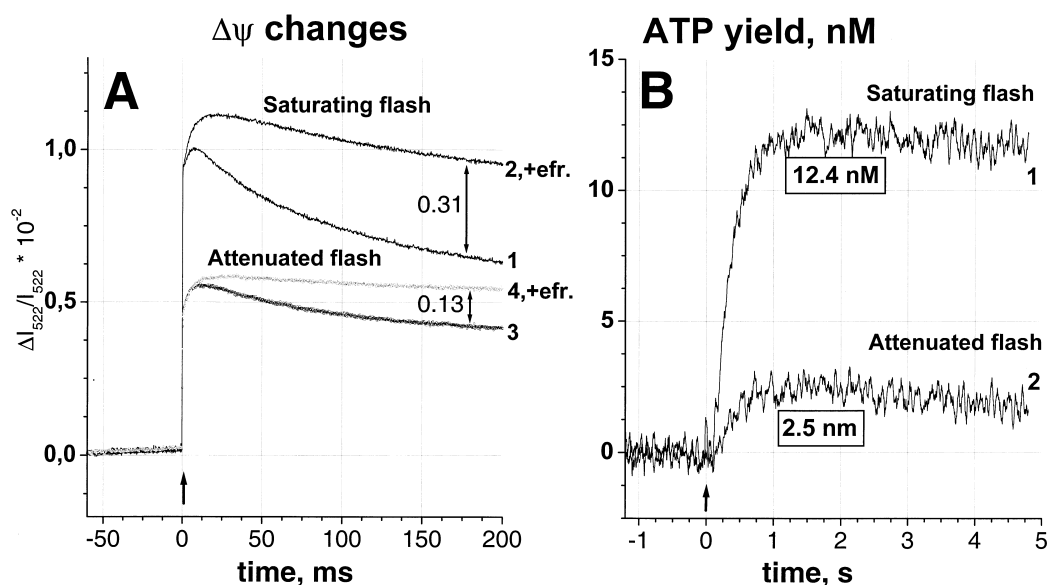


Fig. 3. Impact of the actinic flash attenuation on the ATP synthesis and proton transfer as measured in the same sample. Measuring medium contained 2 mM  $K_2HPO_4$ , 2 mM  $K_4[Fe(CN)_6]$ , 5  $\mu$ M DMF, 2 mM KCN, 5 mM  $MgCl_2$ , 50 mM KCl, 0.3% BSA, 30  $\mu$ M ADP, 8  $\mu$ g/ml luciferase, 0.2 mM luciferin, pH 7.9. Flashes are indicated by arrows. (A) Electrochromic carotenoid bandshift measurements. Solid curves (1 and 2), saturating actinic flash, dotted curves (3 and 4), attenuated actinic flash. 1 and 3, no inhibitors; 2 and 4, +400 nM efrapentin. (B) ATP synthesis in response to an actinic flash (monitored by luciferin–luciferase as indicated in Section 2. 1, saturating flash; 2, attenuated flash. The respective ATP yields are given in boxes.



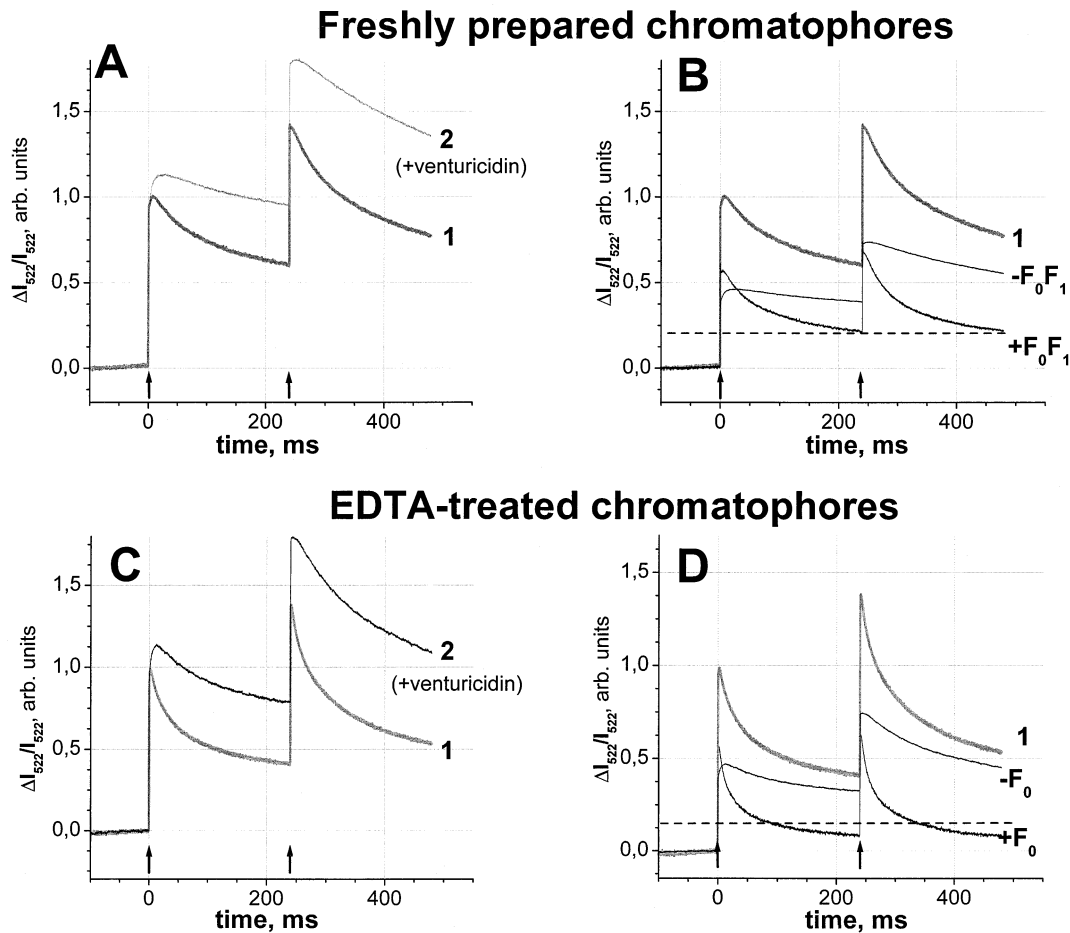


Fig. 4. Assessment of the  $F_0(F_1)$ -lacking chromatophore fraction from the voltage transients generated by two saturating flashes of light fired at 240 ms interval. Arrows indicate actinic flashes. (A) Freshly prepared, coupled chromatophores. Trace 1, ADP 30  $\mu$ M, 2 mM phosphate; trace 2, same as 1, with 200 nM venturicidin added. (B) Reconstruction of kinetics of proton transfer in the  $F_0F_1$ -containing chromatophore population. Trace 1 could be presented as a sum of contributions from the chromatophores lacking the ATP synthase ( $-F_0F_1$  trace=trace 2 multiplied by 0.41, see details in Section 4) and from chromatophores containing the ATP synthase ( $+F_0F_1$  trace=trace 1 minus  $-F_0F_1$  trace). (C) Chromatophores stripped of  $F_1$ . Trace 1, no additions; trace 2, venturicidin to 200 nM. (D) Reconstruction of kinetics of proton transfer in the  $F_0$ -containing chromatophore population. Trace 1 could be presented as a sum of traces for chromatophores lacking  $F_0$  ( $-F_0$  trace=trace 2 multiplied by 0.42, see details in Section 4) and for chromatophores containing  $F_0$  ( $+F_0$ =trace 1 minus  $-F_0$  trace). Dashed horizontal lines represent the estimation of the threshold  $\Delta\psi$  level for the proton transport through the coupled (B) and de-coupled (D) enzyme, respectively. Medium contained 2 mM succinate, 2 mM fumarate, 5  $\mu$ M DMF, 2 mM KCN, 5 mM  $MgCl_2$ , 50 mM KCl, 2 mM  $K_2HPO_4$ , 0.3% BSA, pH 8.0.

ATP synthesis below which no coupled proton transfer could occur [20].

We have noted, however, that when two actinic flashes at 240 ms interval were fired (Fig. 4A), the  $\Delta\psi$  level was substantially greater 200 ms after the second flash than 200 ms after the first one. This difference could be hardly described in the terms of a  $\Delta\psi$  threshold, since the latter is expected to be the same after the first and the second flashes.

A chloroplast thylakoid forms a large electrically

connected system with well over  $10^4$   $F_0F_1$  per thylakoid network with total membrane area of 20–200  $\mu m^2$  [47]). The situation is quite different in the case of much smaller chromatophores with average vesicle surface area of 0.011  $\mu m^2$ . It was conceivable that a fraction of chromatophores totally lacked proton-conducting  $F_0F_1$  or  $F_0$  complexes. To check this possibility, we gave two flashes to the EDTA-treated,  $F_1$ -depleted chromatophores (Fig. 4C,D). The  $\Delta\psi$  threshold for proton transfer through the ‘bare’  $F_0$

in the  $F_1$ -stripped chromatophores is expected to be much lower than in the case of the untreated, coupled ones [14]. Therefore no remarkable contribution from the threshold  $\Delta\psi$  to the overall flash-induced voltage kinetics could be expected. Fig. 4C shows that the fast, 10-ms component of  $\Delta\psi$  decay, attributable to proton flux through  $F_0$ , vanished while considerable  $\Delta\psi$  was still present. This residual  $\Delta\psi$  was again larger after the second flash. This finding could be taken as an evidence for the presence of a chromatophore sub-population that totally lacked proton-conducting  $F_0$ .

From the data in Fig. 4 a rough upper estimate for the relative fraction of such  $F_0(F_1)$ -lacking<sup>1</sup> chromatophores could be obtained by comparing the electrochromic bandshift extents at  $t > 200$  ms in the presence and in the absence of venturicidin. Apparently, the ratio between  $\Delta\psi$  extent at  $t > 200$  ms in the absence of venturicidin and the corresponding  $\Delta\psi$  extent in the presence of inhibitor should correspond roughly to the fraction of the  $F_0$ -lacking chromatophores. It follows from Fig. 4C that up to 50% of the  $F_1$ -stripped chromatophores seemed to lack proton-conducting  $F_0$ . This estimate is quite rough, as the absorbance transients at 522 nm always contained minor contribution from local electrochromic bandshifts, as was mentioned above. A more precise estimate of the  $F_0F_1$ -lacking chromatophore fraction is given in Section 4.

## 4. Discussion

### 4.1. Different types of proton conduction via $F_0F_1$ -ATP synthase

We monitored the flash-induced proton transfer through the  $F_0F_1$ -ATP synthase of *Rb. capsulatus* and the concomitant ATP production with variously treated chromatophore preparations. The greatest ATP yield was found in freshly prepared chromatophores; it decreased by 55% in freeze-stored ( $-80^\circ\text{C}$ ) material and was about zero in the aged material.

The decrease in the ATP yield per flash was proportional to the decrease in the relative extent of the ADP+ $P_i$ -induced, efrapeptin-sensitive component of the proton flow through  $F_0F_1$ . Correspondingly, this component of proton flow could be identified as the catalytic, useful proton flow coupled to the ATP synthesis. The efrapeptin-insensitive but venturicidin-sensitive proton flow was apparently not coupled with the ATP synthesis and could be attributed to the enzyme fraction that lost either the coupling between  $F_0$  and  $F_1$  in the ATP synthase or the  $F_1$  part proper (as with chromatophores that were sonicated in the presence of EDTA). Freezing/thawing, ageing and/or pre-illumination increased the fraction of the de-coupled chromatophores in the absence of ADP.

### 4.2. Estimation of the $H^+/ATP$ ratio. Dependence of the $H^+/ATP$ ratio on the driving force

A single chromatophore vesicle can be approximated by a spherical capacitor with a capacitance of  $4.4 \times 10^{-17}$  F [28,48]. The transmembrane voltage is proportional to the amount of charges transferred across the membrane. As the calibration of carotenoid electrochromic changes in millivolts by diffusion potentials ( $K^+$ /valinomycin) or with other methods of  $\Delta\psi$  measurement, e.g., permeate ion distribution, gave ambiguous results ([21,22,38], see also above), we made no attempt to calibrate  $\Delta\psi$  changes in this work. Instead, we assessed the amount of charges that were translocated by  $F_0F_1$  by using the charge transfer by the RCs as a reference. On average, 1.1 charges were transferred across the membrane by each RC in response to our 10  $\mu\text{s}$  flash (see Section 2). We assumed that the extent of the very fast, here unresolved, increase in  $\Delta\psi$  (see Fig. 3B) was equivalent to the translocation of 1.1 charge per reaction center (1.1 eq/mol RC).

We assumed that only the efrapeptin-sensitive charge transfer through a functional ATP synthase was coupled to the ATP synthesis (see above). The extent of the efrapeptin-sensitive component (see Fig. 3B and the corresponding comments in the text) was calibrated in charges transferred per reaction center by comparison with the extent of voltage transients corresponding to the charge separation in the RC. Both the concentration of RCs in the sample and the amount of the ATP synthesized could be rather

<sup>1</sup> Hereafter we define for simplicity a proton conducting ATP synthase moiety as  $F_0(F_1)$  independently, whether it is coupled or not.

reliably determined, as described in Section 2. Such estimates of the  $H^+/ATP$  ratio under ‘flash-induced’ ATP synthase operation mode can be considered as complementary to those obtained for the enzyme under the steady state turnover conditions.

We calculated the  $H^+/ATP$  ratio as

$$H^+/ATP = \frac{A \times C_{RC}}{C_{ATP}}$$

where  $A$  is the extent of efrapentin-sensitive component (in charges transferred per reaction center),  $C_{RC}$  is the concentration of reaction centers in the sample, and  $C_{ATP}$  is the increase in ATP concentration after an actinic flash. The ratio  $H^+/ATP$  for a single saturating actinic flash calculated for six different samples in the way described was  $3.3 \pm 0.6$ . We found out that when the actinic flash was attenuated so that the initial transmembrane voltage decreased by a factor of 2.4, the extent of the  $ADP+P_i$ -sensitive proton transfer through  $F_0F_1$  decreased by factor of about 2.8, whereas the ATP yield dropped about 4.3-fold (see Table 1). This implied an increase in the  $H^+/ATP$  ratio from  $3.3 \pm 0.6$  to  $5.1 \pm 0.9$ .

The higher  $H^+/ATP$  ratio after weak flash was unlikely to be due to the larger relative contribution from the ATP hydrolysis. The post-flash hydrolysis of ATP, due to the activity both of the coupled and de-coupled  $F_1$  molecules and of luciferase proper, was negligibly slow even on a time scale of seconds (see Materials and Methods). The most probable reason of such a slow ATP consumption was the small ATP amount in the sample and relatively high ADP concentration.

Other possible reasons for the revealed dependence of the  $H^+/ATP$  ratio on the driving force are listed below.

1. The partial blockage of the cytochrome- $bc_1$  complex by high  $\Delta\tilde{\mu}_{H^+}$  when the proton escape from chromatophores through ATP synthase was inhibited by venturicidin or efrapentin. Such blockage would be more pronounced at higher  $\Delta\tilde{\mu}_{H^+}$  after a saturating flash and could lead to an underestimation of genuine  $H^+/ATP$  ratio. Our preliminary estimates indicate, however, that this effect is pronounced at acidic pH (less than 7) and after the second flash. Therefore it could hardly account alone for the *whole* observed difference in  $H^+/$

ATP ratios. A radical solution could be to measure the dependence of the  $H^+/ATP$  ratio on the driving force with completely inhibited cytochrome- $bc_1$  complex. Unfortunately, the protons that are released by the latter seem to be crucial for the ATP synthesis, so that the ATP yield in the presence of myxothiazol is hardly measurable even after a saturating light flash [49].

2. Activation of the *Rb. capsulatus*  $F_0F_1$  by  $\Delta\psi$ , as described by Turina et al. [37]. One possibility is that the initial ‘activating’ proton transfer through  $F_0F_1$  leads to the ATP release from the tight-binding site and is thereby ‘catalytic’. In such a case no influence on the  $H^+/ATP$  ratio could be expected. If, however, the initial ‘activating’ proton transfer is not coupled with the ATP release and precedes the transfer of the ‘catalytic’ protons (as discussed in [50]), it could lead to the increase in the  $H^+/ATP$  ratio. As the lifetime of an ‘activated’ ATP synthase is in the order of tens of seconds [37], we tried our best to keep the  $F_0F_1$ -ATP synthase activated throughout the measurement (see Section 2). However, if some ‘activation’ component of proton transfer remained, then it was expected to be higher after the weak flash, because then the  $\Delta\psi$  level was lower. In such a case the apparent  $H^+/ATP$  ratio would also be higher after the weak flash.
3. Elasticity of the power transmission in ATP synthase. The current mechanistic models [2,13,14] propose that the  $c$ -ring rotates in such way that  $c$ -subunit carboxyls slide along the  $a$ -subunit one by one [51]. Protons that are picked from one side are released one by one to the other side of the membrane. In such a case, each proton translocated causes rotation of the  $c$ -ring by a certain angle increasing the elastic strain of the enzyme until enough energy is accumulated to drive ATP release from  $F_1$ . The torsional strain is built up in discrete angular steps as driven by subsequent proton transfer events in  $F_0$ . The  $\Delta\tilde{\mu}_{H^+}$ -driven proton translocation, from the first to the last step, has to operate then against increasing back-pressure. When  $\Delta\tilde{\mu}_{H^+}$  is not high enough to drive the last proton that is needed to synthesize one ATP molecule (i.e., after a weak flash), the initial

protons might be still transferred through  $F_1F_0$ . Their transfer would not be accompanied by ATP release. This might be the case in our experiments. Under excitation with the weak flash the ATP concentration after the flash increased by 2.5 nM only (Fig. 3A). This was below the estimated total concentration of ATP synthase in our samples (approx. 10–20 nM). Apparently, that under such conditions there was less than one ATP molecule synthesized per enzyme.

As well, one cannot completely rule out the physical possibility that the  $H^+$ /ATP ratio might vary with the driving force, although we do not see a way to accommodate it with the current mechanistic models of proton transfer through  $F_0$ . Further experiments are necessary to discriminate between the listed possibilities.

#### 4.3. $F_0(F_1)$ -lacking chromatophore fraction

As noted in Section 3, about 50% of chromatophores seemed to lack proton-conducting  $F_0(F_1)$ . In agreement with this finding, the number of ATP synthases per vesicle in the rest of chromatophores seems to be very small as well. Such a conclusion follows from the observation that the kinetics both of the coupled and of the de-coupled proton transport overlap as measured in differently treated chromatophore preparations (see Fig. 1C,F). If a large amount of  $F_0F_1$  were present per each chromatophore, then the gradual de-coupling of the ATP synthase (e.g., by freezing/thawing or EDTA-treatment) should lead to the acceleration of the de-coupled proton transfer, because an increasing number of 'unrestricted' proton exits per each chromatophore appeared. It is relevant that the appearance of at least one de-coupled  $F_0(F_1)$  in a given vesicle would switch off the coupled proton transfer. The de-coupled enzyme is expected to transport most of the protons because of its lower thermodynamic threshold and faster transfer rate. That would leave the coupled enzyme undetectable by the method applied. As neither of these effects was pronounced, we can conclude that each chromatophore carried just a few, if any,  $F_0F_1$ -ATP synthases. Physiologically such a small number of functional  $F_0F_1$  per chroma-

tophore would not matter for the cell where all chromatophores form a contiguous membrane system.

The detection of a  $F_0F_1$ -lacking chromatophore fraction rationalizes an earlier observation that the chromatophore suspension depleted from  $F_1$  was still able to maintain a relatively large level of  $\Delta pH$  [33] and  $\Delta\psi$  [52]. As well, the presence of a  $F_0F_1$ -lacking chromatophore fraction corresponds nicely to a very interesting observation of Crimi and co-workers [38] that the extent of carotenoid bandshift induced by the ATP hydrolysis after addition of ATP to *Rb. capsulatus* chromatophores was much smaller ( $\sim 70$  mV, as calibrated by the  $K^+$ /valinomycin routine), than the  $\Delta\psi$ -threshold of the ATPase activation (100–150 mV). Exactly this result could be expected if about half of all the chromatophores had no ATP synthase at all. As the observed carotenoid bandshift represents the weighted sum of voltage transients in a heterogeneous ensemble of vesicles, no ATP-induced carotenoid bandshift should occur in this  $F_0F_1$ -lacking chromatophore fraction. These chromatophores should, however, respond by carotenoid bandshift both to the  $K^+$ /valinomycin addition and to illumination.

The presence of an  $F_0(F_1)$ -lacking chromatophore fraction calls for reconciliation of the role of proton slip in chromatophores of *Rb. capsulatus*. In our previous report we have attributed the proton transfer through  $F_0F_1$  in the absence of  $ADP+P_i$  to the proton slip [20]. The reason for this attribution was a large residual  $\Delta\psi$  that was still present even when the fast component of proton transfer via the ATP synthase was complete (see above). By analogy with chloroplast thylakoids [46], we have speculated that above a certain  $\Delta\psi$  threshold protons could slip through the coupled ATP synthase in the absence of ADP and phosphate. In the view of new data, we see a more complex relation between the futile proton transfer and the proton slip in chromatophores of *Rb. capsulatus*. Currently this relation could be understood in the following way: the conformational state of the  $F_0F_1$  complex in the absence of its physiological substrates, namely ATP/ADP and  $P_i$ , seems to be metastable, at best. If it is not stabilized by the addition of ADP/ATP and  $P_i$ , a gradual de-coupling of  $F_0$  and  $F_1$  develops. The de-coupling could be accelerated by treatments of different nature, e.g., by freezing/thawing, ageing, or illumina-

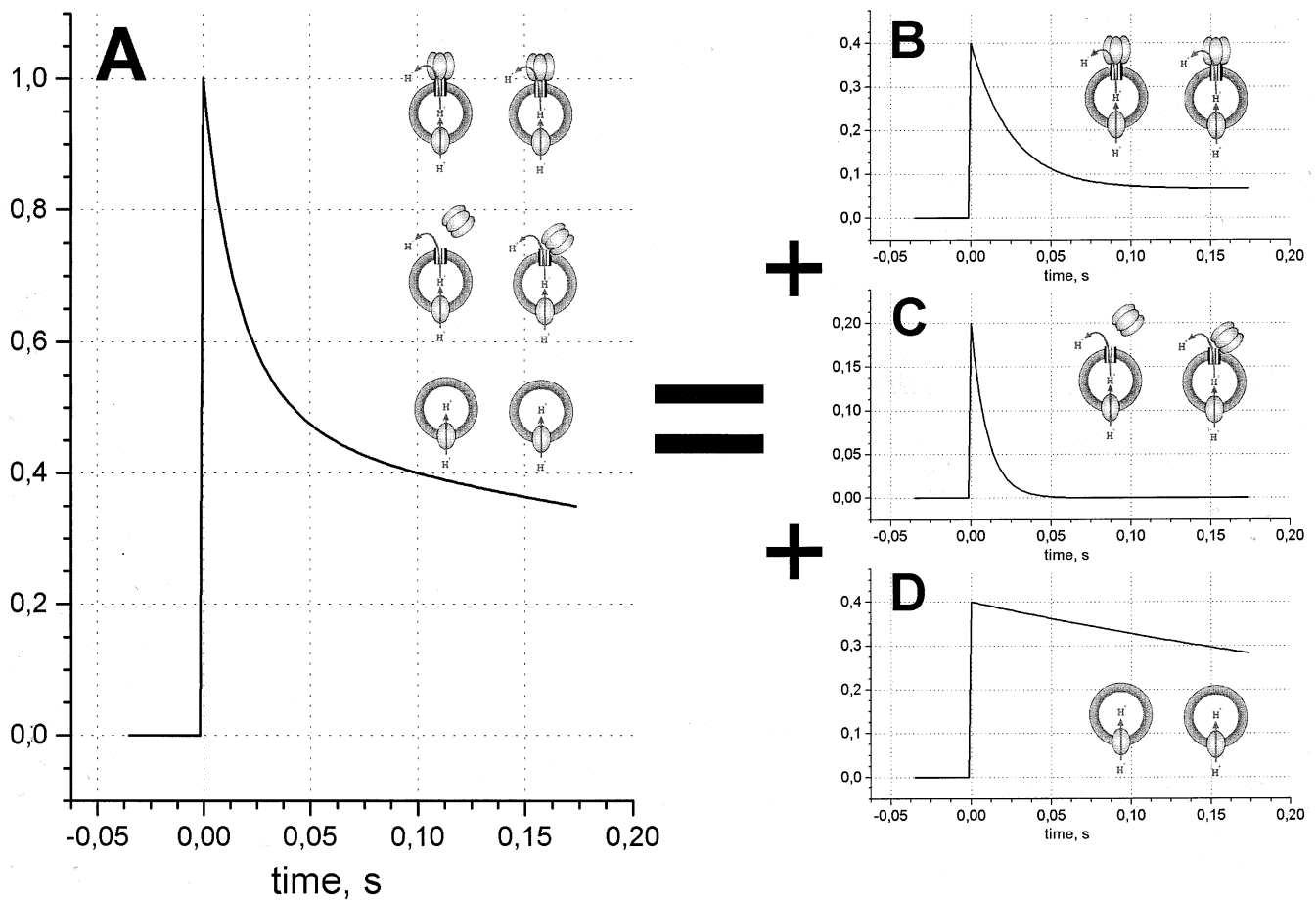


Fig. 5. Scheme of the voltage discharge in a typical suspension of *Rb. capsulatus* chromatophores. A schematic picture of chromatophores with a ' $\Delta\tilde{\mu}_{H^+}$  generator' and  $F_0(F_1)$  in an appropriate functional state is given in the upper left corner of each graph. The measured trace A is the sum of traces: B represents the chromatophore fraction with active  $F_0F_1$ , decay time 25 ms, the trace being scaled here by a factor of 0.4; C represents the chromatophore fraction with damaged, uncoupled  $F_0F_1$ , decay time 10 ms, the trace being scaled by a factor of 0.2; D represents the chromatophore fraction without active ( $F_0$ ) $F_1$ , decay time 320 ms, the trace being scaled by a factor of 0.4.

tion. The increase in the extent of the futile proton transfer after pre-illumination (Fig. 2) suggests that  $\Delta\tilde{\mu}_{H^+}$  that is built in the absence of  $ADP+P_i$  upon illumination drives protons through a coupled  $F_0F_1$  (see [53] for a description of related phenomena in the chloroplast ATP synthase). Such a proton transfer through  $F_0F_1$  that apparently leads, although with an unknown quantum yield, to the de-coupling of the enzyme can be defined as a proton slip. After the enzyme is de-coupled, proton transfer becomes futile. The de-coupling by illumination was initially reversible, so that the enzyme activity could be restored by a prompt addition of nucleotides and  $P_i$  (see Fig. 2). In chromatophores that were partly de-coupled by freezing/thawing, we also observed some

functional reversal after their long incubation in the presence of nucleotides and  $P_i$ .

#### 4.4. Deconvolution of electrochromic transients

Thus, there were always three subsets of chromatophores in our samples, namely: those with coupled  $F_0F_1$ , those with at least one proton conducting but de-coupled  $F_0$ , and the  $F_0(F_1)$ -lacking ones. Therefore, each kinetic transient was a composition of three traces, as illustrated in Fig. 5. The kinetics of the carotenoid bandshift in the population of the  $F_0(F_1)$ -lacking chromatophores was expected to be similar to those in the presence of venturicidin, when the charge transfer through  $F_0$  was blocked. This

allowed deconvoluting the cumulative electrochromic transient into the contributions from the  $F_0(F_1)$ -containing and  $F_0(F_1)$ -lacking chromatophore fractions as follows. Let  $x$  be the fraction of the  $F_0(F_1)$ -lacking chromatophores,  $\Delta\psi_{\text{Cond1}}$  and  $\Delta\psi_{\text{Cond2}}$  be the  $\Delta\psi$  values in the absence of an  $F_0(F_1)$  inhibitor at  $t=200$  ms after the first and the second actinic flash, respectively, and  $\Delta\psi_{\text{Vent1}}$  and  $\Delta\psi_{\text{Vent2}}$  the corresponding  $\Delta\psi$  values in the presence of the inhibitor. In the presence of venturicidin all chromatophores in the sample behave in the same way: no proton transfer through ATP synthase occurs. In the absence of inhibitors only fraction  $x$  behaves this way. Its contribution to the overall  $\Delta\psi$  will be  $x\Delta\psi_{\text{Vent}}$ . The contribution of the residual fraction  $(1-x)$  of chromatophores that contain  $F_0F_1$  will be  $\Delta\psi_{\text{Cond}} - x\Delta\psi_{\text{Vent}}$  by definition. As it is assumed that  $\Delta\psi$  in the  $F_0(F_1)$ -containing chromatophores drops to a threshold value that is same at  $t=200$  ms after the first and the second flash (see Section 3), we get  $\Delta\psi_{\text{Cond1}} - x\Delta\psi_{\text{Vent1}} = \Delta\psi_{\text{Cond2}} - x\Delta\psi_{\text{Vent2}}$  from which it follows that

$$x = \frac{\Delta\psi_{\text{Cond1}} - \Delta\psi_{\text{Cond2}}}{\Delta\psi_{\text{Vent1}} - \Delta\psi_{\text{Vent2}}}$$

Application of the latter relation to the fresh chromatophore preparation data presented in Fig. 4A gives about 41% of the  $F_0(F_1)$ -lacking chromatophores; same treatment of the data on chromatophores stripped from  $F_1$  in Fig. 4B gives 42% of  $F_0(F_1)$ -lacking chromatophores. Similarity of the fraction of  $F_0(F_1)$ -lacking chromatophores in two differently treated chromatophore preparations shows that the absence of  $F_0$  conduction is a genuine property of a given chromatophore vesicle and, unlike the de-coupling between  $F_0$  and  $F_1$ , is not induced by sonication/ageing/EDTA treatment. After quantifying the  $F_0(F_1)$ -lacking chromatophore fraction, we re-analyzed our kinetic data of the last few years for the extent of this fraction in other chromatophore preparations. The fraction seemed to vary around 40% and hence seems to be independent either of the chromatophore disruption protocol (French-press treatment versus sonication) or of the chromatophore preparation medium. All our chromatophore preparations were, however, obtained from cells grown under the same conditions. So far, we used cells of *Rb. capsulatus* that

were grown at the same bench and at an illumination of 15–30 W/m<sup>2</sup> and were harvested at the end of the logarithmic growth phase. Therefore, we cannot exclude that the extent of  $F_0(F_1)$ -lacking chromatophore fraction may depend on the cell growth regime or on the harvesting stage. We intend to check these possibilities in the nearest future.

Knowing the fraction of the  $F_0(F_1)$ -lacking chromatophores, it is possible to ‘extract’ the picture of  $\Delta\psi$  changes in the  $F_0F_1$ -containing chromatophores simply by subtracting the trace obtained in the presence of venturicidin scaled by a respective factor, i.e., 0.41 or 0.42 in two given cases, from the original traces in Fig. 4A,C. We made this deconvolution both for data on the coupled chromatophores in Fig. 4A and for data on the  $F_1$ -depleted ones in Fig. 4C. The respective traces are shown in Fig. 4B,D, correspondingly. It is clearly seen that  $\Delta\psi$  threshold for the proton flow through coupled  $F_0F_1$  is substantially higher than for the ‘bare’  $F_0$  (dashed lines in Fig. 4B,D), in accordance with thermodynamics expectations.

## Acknowledgements

Very helpful discussions with Professors B.J. Jackson and B.-A. Melandri are appreciated. This work has been supported in part by the Alexander von Humboldt Foundation and by grants from the Deutsche Forschungsgemeinschaft (Mu-1285/1, Ju-97/13, 436-RUS-113/210).

## References

- [1] P.D. Boyer, Ann. Rev. Biochem. 66 (1997) 717–749.
- [2] W. Junge, H. Lill, S. Engelbrecht, Trends. Biochem. Sci. 22 (1997) 420–423.
- [3] J. Weber, A.E. Senior, Biochim. Biophys. Acta 1458 (2000) 300–309.
- [4] G. Deckers-Hebestreit, J. Greie, W. Stalz, K. Altendorf, Biochim. Biophys. Acta 1458 (2000) 364–373.
- [5] S.D. Dunn, D.T. McLachlin, M. Revington, Biochim. Biophys. Acta 1458 (2000) 356–363.
- [6] E. Muneyuki, H. Noji, T. Amano, T. Masaike, M. Yoshida, Biochim. Biophys. Acta 1458 (2000) 467–481.
- [7] H. Seelert, A. Poetsch, N.A. Dencher, A. Engel, H. Stahlberg, D.J. Muller, Nature 405 (2000) 418–419.

- [8] T.M. Duncan, V.V. Bulygin, Y. Zhou, M.L. Hutcheon, R.L. Cross, *Proc. Natl. Acad. Sci. USA* 92 (1995) 10964–10968.
- [9] Y. Zhou, T.M. Duncan, R.L. Cross, *Proc. Natl. Acad. Sci. USA* 94 (1997) 10583–10587.
- [10] D. Sabbert, S. Engelbrecht, W. Junge, *Nature* 381 (1996) 623–626.
- [11] H. Noji, R. Yasuda, M. Yoshida, K. Kinosita, *Nature* 386 (1997) 299–302.
- [12] H.Y. Wang, G. Oster, *Nature* 396 (1998) 279–282.
- [13] P. Dimroth, H. Wang, M. Grabe, G. Oster, *Proc. Natl. Acad. Sci. USA* 96 (1999) 4924–4929.
- [14] D.A. Cherepanov, A.Y. Mulkidjanian, W. Junge, *FEBS Lett.* 449 (1999) 1–6.
- [15] J.B. Jackson, S. Saphon, H.T. Witt, *Biochim. Biophys. Acta* 408 (1975) 83–92.
- [16] K.M. Petty, J.B. Jackson, *Biochim. Biophys. Acta* 547 (1979) 463–473.
- [17] B.A. Melandri, G. Venturoli, A. De Santis, A. Baccarini-Melandri, *Biochim. Biophys. Acta* 592 (1980) 38–52.
- [18] A.R. Crofts, C.A. Wraight, *Biochim. Biophys. Acta* 726 (1983) 149–185.
- [19] W. Junge, *Proc. Natl. Acad. Sci. USA* 84 (1987) 7084–7088.
- [20] B.A. Feniouk, D.A. Cherepanov, W. Junge, A.Y. Mulkidjanian, *FEBS Lett.* 445 (1999) 409–414.
- [21] A.J. Clark, J.B. Jackson, *Biochem. J.* 200 (1981) 389–397.
- [22] M. Symons, C. Swysen, C. Sybesma, *Biochim. Biophys. Acta* 462 (1977) 706–717.
- [23] W. Ausländer, W. Junge, *FEBS Lett.* 59 (2) (1975) 310–315.
- [24] S. Saphon, J.B. Jackson, H.T. Witt, *Biochim. Biophys. Acta* 408 (1975) 67–82.
- [25] A.Y. Mulkidjanian, W. Junge, *FEBS Lett.* 353 (1994) 189–193.
- [26] A. Lundin, A. Thore, M. Baltscheffsky, *FEBS Lett.* 79 (1977) 73–76.
- [27] H. Lill, W. Junge, *Eur. J. Biochem.* 179 (1989) 459–467.
- [28] S. Saphon, J.B. Jackson, V. Lerbs, H.T. Witt, *Biochim. Biophys. Acta* 408 (1975) 58–66.
- [29] A.R. Crofts, M. Guergova-Kuras, S. Hong, *Photosynth. Res.* 55 (1998) 357–362.
- [30] J. Lascelles, *Biochem. J.* 72 (1959) 508–518.
- [31] R.K. Clayton, in: H. Gest, A. San Pietro, L.P. Vernon (Eds.), *Bacterial Photosynthesis*, Antioch Press, Yellow Springs, 1963, pp. 495–500.
- [32] A.Y. Mulkidjanian, M.D. Mamedov, L.A. Drachev, *FEBS Lett.* 284 (1991) 227–231.
- [33] B.A. Melandri, A. Baccarini-Melandri, A. San Pietro, H. Gest, *Proc. Natl. Acad. Sci. USA* 67 (1970) 477–484.
- [34] A. Baccarini-Melandri, H. Gest, A. San Pietro, *J. Biol. Chem.* 245 (1970) 1224–1226.
- [35] B.A. Melandri, A. Baccarini-Melandri, A. San Pietro, H. Gest, *Science* 174 (1971) 514–516.
- [36] W. Junge, in: T.W. Goodwin (Ed.), *Chemistry and Biochemistry of Plant Pigments*, 2nd Edition, Vol. 2, Academic Press, London, 1976, pp. 233–333.
- [37] P. Turina, B. Rumberg, B.A. Melandri, P. Gräber, *J. Biol. Chem.* 267 (1992) 11057–11063.
- [38] M. Crimi, V. Fregni, A. Altimari, B.A. Melandri, *FEBS Lett.* 367 (1995) 167–172.
- [39] J.B. Jackson, A.R. Crofts, *Eur. J. Biochem.* 120 (1971) 120–130.
- [40] D.M. Tiede, L. Utschig, D.K. Hanson, D.M. Gallo, *Photosynth. Res.* 55 (1998) 267–273.
- [41] J.B. Jackson, in: C. Anthony, (Ed.), *Bacterial Energy Transduction*, Academic Press, London, 1988, pp. 317–376.
- [42] J.P. Abrahams, S.K. Buchanan, M.J. van Raaij, I.M. Fearnley, A.G. Leslie, J.E. Walker, *Proc. Natl. Acad. Sci. USA* 93 (1996) 9420–9424.
- [43] M. von Brufani, W. Keller-Schierlein, W. Löffler, I. Mansperger, H. Zähner, *Helv. Chim. Acta* 51 (1968) 1293–1304.
- [44] P.E. Linnett, R.B. Beechey, *Methods Enzymol.* 55 (1979) 472–518.
- [45] L. Slooten, S. Vandenbranden, *Biochim. Biophys. Acta* 976 (1989) 150–160.
- [46] W. Junge, *Eur. J. Biochem.* 14 (1970) 582–592.
- [47] G. Schonknecht, G. Althoff, W. Junge, *FEBS Lett.* 277 (1990) 65–68.
- [48] N.K. Packham, J.A. Berriman, J.B. Jackson, *FEBS Lett.* 89 (1978) 205–210.
- [49] B.A. Feniouk, D.A. Cherepanov, W. Junge, A.Y. Mulkidjanian, *EBEC Short Rep.* 11 (2000) 213.
- [50] G. Groth, W. Junge, *FEBS Lett.* 358 (1995) 142–144.
- [51] O. Panke, K. Gumbiowski, W. Junge, S. Engelbrecht, *FEBS Lett.* 472 (2000) 34–38.
- [52] B.A. Melandri, A. Baccarini-Melandri, A.R. Crofts, R.J. Cogdell, *FEBS Lett.* 24 (1972) 141–145.
- [53] S. Ponomarenko, I. Volfson, H. Strotmann, *FEBS Lett.* 443 (1999) 136–138.